Competing dissociation channels in the photolysis of S_2Cl_2 at 235 nm

Tina S. Einfeld, Christof Maul, and Karl-Heinz Gericke[a)]
Institut für Physikalische und Theoretische Chemie, Technische Universität Braunschweig, Hans-Sommer-Strasse 10, D-38106 Braunschweig, Germany

Alexei Chichinin
Institut für Physikalische und Theoretische Chemie, Technische Universität Braunschweig, Hans-Sommer-Strasse 10, D-38106 Braunschweig, Germany and Institute of Chemical Kinetics and Combustion, 630090 Novosibirsk, Russia

(Received 15 January 2002; accepted 5 June 2002)

The photodissociation of disulfur dichloride (S_2Cl_2) at 235 nm has been studied by three-dimensional (3D) imaging of the chlorine product recoil in its ground state $^2P_{3/2}$[Cl] and excited spin–orbit state $^2P_{1/2}$[Cl*] employing the resonance enhanced multiphoton ionization and time-of-flight techniques. The photodissociation proceeds mainly along the three channels forming S_2+2Cl (1), S_2Cl+Cl (2), and 2 SCl (3) photoproducts where slow and fast Cl fragments are released in (1) and (2), respectively. The relative yield of channel (1) with respect to channel (2) was determined to be 1.2:1.0. The yield of Cl*, $\phi(Cl^*)=P(Cl^*)/[P(Cl)+P(Cl^*)]$, was found to be 0.35. The obtained state-specific velocity distributions of Cl and Cl* are mainly different in the high energy range: For Cl* the two dissociation channels are almost equally present, whereas in the case of ground state Cl the contribution of dissociation channel (2) is of minor importance. The dependence of the anisotropy parameter β on the fragment recoil velocity was directly determined due to the novel technique where the 3D momentum vector of a single reaction product is observed. For both spin–orbit states the anisotropy parameters differ for slow, intermediate, and fast chlorine atoms. The observed β values change from zero to slightly negative values up to positive values with increasing kinetic energy. These observations can be explained by two overlapping dissociation channels, where the two-body channel (2) releases the chlorine atom with high kinetic energy and a positive β parameter via an excited ^1A state, whereas the three-body channel (1) proceeds mainly sequentially, where the first Cl atom is released with intermediate speed and a slightly negative β value via an excited ^1B state, while the second Cl product atom in the decay of S_2Cl is released isotropically with slow recoil velocities. © *2002 American Institute of Physics.*
[DOI: 10.1063/1.1496465]

I. INTRODUCTION

The UV absorption spectrum of S_2Cl_2,[1–3] shown in Fig. 1, starts at a wavelength of 350 nm with a first maximum around 300 nm followed by a broad absorption peak at 260 nm. The broad continuum is attributed to the $n\rightarrow\pi^*_{S-S}$ and the $n\rightarrow\sigma^*_{S-Cl}$ transition, where the nonbonding orbitals can be located at the S or the Cl atoms. Below 230 nm, another absorption band starts to rise which has not yet been assigned.[2] The ground state of S_2Cl_2 is of C_2 symmetry as determined by electron diffraction and is shown in Fig. 2.[4]

The photolysis of the S_2Cl_2 molecule has been the subject of several experimental investigations for decades covering the whole spectral range from 110 to 514 nm.[5–12] The following dissociation channels were observed:

$$S_2Cl_2\rightarrow S_2+Cl+Cl, \quad (1)$$

$$S_2Cl_2\rightarrow S_2Cl+Cl, \quad (2)$$

$$S_2Cl_2\rightarrow 2SCl, \quad (3)$$

$$S_2Cl_2\rightarrow SCl_2+S. \quad (4)$$

Tokue *et al.*[5] studied the photoabsorption cross section and the fluorescence excitation spectrum of S_2Cl_2 vapor in the range 110–200 nm using synchrotron radiation. They assigned a number of broad bands in the 120–170 nm region as Rydberg transitions. The predominant photodissociation process in the 120–155 nm region was the three-body decay (1),[13] where S_2Cl_2 splits into three photofragments. Chasovnikov *et al.*[6] observed atomic Cl fragments at a dissociation wavelength of 266 nm by laser magnetic resonance while Tiemann *et al.*[7] studied the SCl radical generated by the photolysis at 248 nm by infrared diode laser spectroscopy. It was found that the photolysis yields the SCl radical in its electronic ground state via channel (3). Later Park *et al.*[8] studied the photodissociation of S_2Cl_2 at 308, 248, and 193 nm where the radical channel (2) was observed. In addition, Park *et al.*[14] used the photolysis of S_2Cl_2 at 248 nm as a source of Cl radicals to study the reaction dynamics of chlorine atoms with deuterated cyclohexane. The radical decay channel (2) was confirmed by Lee *et al.*[9] by translational spectroscopy at 308 nm. It was observed that S_2Cl_2 dissociates via channel (2) with a mean translational energy $\langle E_T\rangle$ of 65 kJ/mol and the measured anisotropy parameter β was 0.4 $\pm$0.2. Lee *et al.* concluded that S_2Cl_2 undergoes a fast dis-

[a)]Author to whom all correspondence should be addressed.

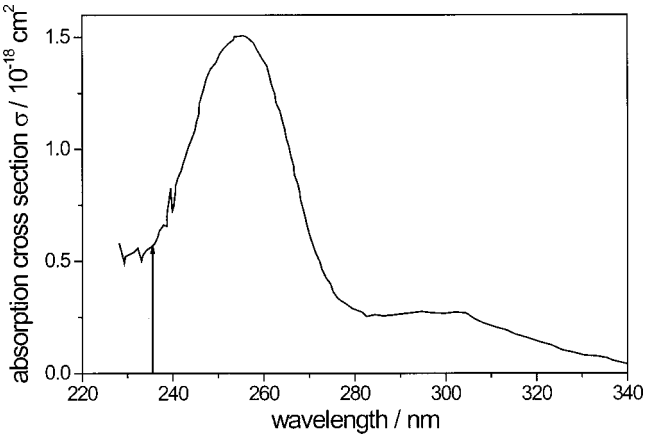

FIG. 1. Absorption cross section of S_2Cl_2 based on the publication of Speth *et al.* (Ref. 1). The wavelength used in the present experiment is marked by an arrow.

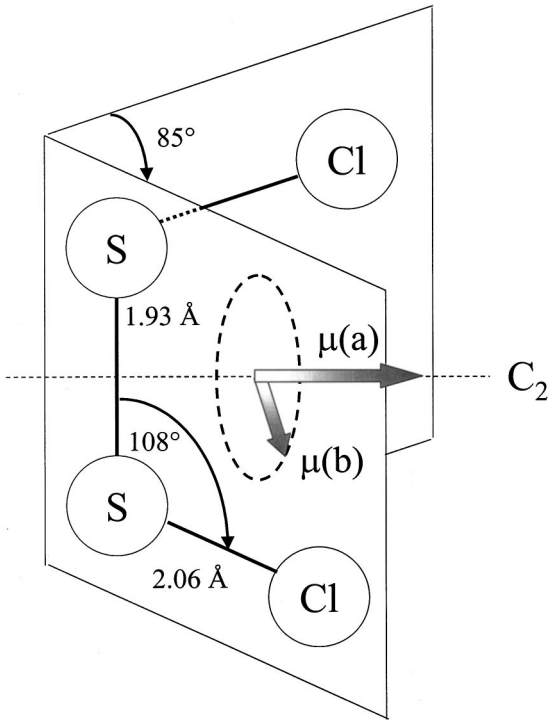

FIG. 2. Structure of S_2Cl_2 (Ref. 2) and the geometry of both transition dipole moments μ(a) parallel to the symmetry axis C_2 and μ(b) lying in the plane perpendicular to the C_2 axis.

sociation process after excitation via a parallel transition. However, the interest in the photodissociation of S_2Cl_2 exceeded the UV region, as Chiu and Chang[10] studied the resonance Raman and fluorescence spectra of the S_2Cl radical which was generated by the photodissociation of S_2Cl_2 using 514.5 nm laser radiation. They confirmed that the radical channel (2) dominates at 514.5 nm, which is also the case in the photodissociation at 308 nm.

Recent work includes two studies by Tiemann and co-workers.[11,12] Lindner *et al.*[11] studied the major dissociation channels of S_2Cl_2 in the range between 280 and 240 nm by using laser induced fluorescence and resonance enhanced multiphoton ionization and time-of-flight techniques (REMPI-TOF) detection techniques on the state-specific photofragments S and S_2. They concluded that the high-energy edge of the main absorption maximum is mainly the result of a fragmentation either into S_2+Cl_2, where Cl_2 is in the $^3\Pi$ state, or into S_2+2Cl (1). The long wavelength part of the absorption spectrum is connected to the channel S_2Cl+Cl (2) and toward shorter wavelength a complex competition between different dissociation channels is expected. The involvement of SCl as an intermediate product is less favorable. In addition to the above-described channel, the dissociation into SCl_2+S along channel (4) was observed.

Lee *et al.*[12] studied the photodissociation of S_2Cl_2 at 248 and 193 nm by translational spectroscopy. The SCl product was detected with a relative yield of 20%. Due to the measured anisotropy parameter β_{SCl} of 1.6 at 248 nm and 0.6 at 193 nm, they concluded that a rapid S–S bond fission takes place on the excited ^1B state. Lee *et al.* observed that the S–Cl bond fission is predominant with a factor 3.0 higher than the S–S bond fission. Via reaction (2) two separate product Cl atom translational energy distributions of $\langle E_T \rangle = 42$ and 126 kJ/mol were found. The slow S_2Cl fragments undergo a secondary dissociation to form isotropically distributed S_2 and Cl which probably arise from the S_2Cl ground electronic state, whereas the fast components more likely originate from a mixed excitation of ^1A and ^1B states of S_2Cl_2. In addition, they observed the dissociation channel (4). At 193 nm the three-body decay channel (1) becomes more efficient forming S_2 and 2Cl with a Cl atom translational energy distribution of $\langle E_T \rangle = 42$ kJ/mol, which is in agreement with the value derived by Park *et al.*[8] However, the former interpretation given by Park that the observed Cl are released via a radical channel at 193 nm was misleading. The observed β_{Cl} value of -0.3 hints at an involvement of a higher ^1B state in the excitation.

The former studies show that the dissociation of S_2Cl_2 following absorption in the main band between 230 and 280 nm is a highly complex process involving several excited potential energy surfaces and all decay channels (1)–(4) are in competition with each other. In order to elucidate the dynamics behind this complicated behavior more detailed experimental data are required. Since we are able to observe the three-dimensional (3D) momentum vector of a single state-selective photofragment by applying a novel 3D imaging technique[15,16] the unsolved questions in the photodissociation of S_2Cl_2 are a promising task to study. There are the relative yield of the reactions, the spin–orbit branching ratio of Cl*/Cl, the translational energy disposal, the different involved upper states, and the mechanism of the decay. To this end, the energy dependence of the anisotropy parameter β is the most valuable tool to analyze the dissociation process including the dissociation energy $D_0(ClS_2-Cl)$.

II. EXPERIMENT

A more detailed description of the experimental setup and the novel position sensitive detector (PSD) has been published elsewhere.[15,16] Briefly, it consists of a combination of a home-built single-field time-of-flight (TOF) mass spec-

trometer and a position sensitive detector.[17–19] The spectrometer was evacuated to a base pressure of $\sim 10^{-8}$ mbar by a turbomolecular pump system. Disulfur dichloride was constantly cooled to -10 °C (gas pressure: ~ 1 mbar at -10 °C) to prepare a mixture of 0.03% S_2Cl_2 in helium which was flowing through the cooling vessel. Measurements of the room temperature sample were performed at a pressure of 10^{-7} mbar, corresponding to a S_2Cl_2 density of $10^6/cm^3$. Measurements of jet-cooled samples at a temperature of 8 K agree with the results from the bulk measurements, but were not further analyzed due to background interference.

Simultaneous dissociation and state-selective detection of chlorine atoms were performed using one dye laser pumped by a Nd:YAG laser (Coherent, Infinity 40 100). The dye laser (Lambda Physik, Scanmate) was operated with Coumarin 47 at a repetition rate of 100 Hz, its light was frequency-doubled by a BBO crystal and focused by a 20 cm lens in order to decrease the reaction volume to 5×10^{-4} mm^3. The output window was arranged in a Brewster angle configuration of 54° to reduce the internally reflected light. The energy of the frequency-doubled light amounted to 5–10 μJ per pulse. The energy was kept low to obtain approximately one fragment signal per ten laser pulses to avoid kinetic energy transfer to the fragments due to space charge effects and saturation of the dissociation step. The laser beam, the molecular beam, and the detector axes were mutually orthogonal in the interaction region. Ultimate care was taken to overlap the light and the molecular beam which was checked frequently by monitoring of NO via (1+1) REMPI at 226 nm and optimization of the signal intensity.[20] The polarization of the laser was changed by a half wave plate in order to investigate the spatial fragment distribution. Typically the acceleration voltage was 800 V in the acceleration tube of the TOF spectrometer corresponding to an acceleration field of 16 kV/m.

The ^2P_J state of the chlorine atom is split by 882 cm^{-1} due to spin–orbit coupling into $Cl(^2P_{3/2})$ and $Cl^*(^2P_{1/2})$. Both states were detected by a (2+1) REMPI process. The ground state was probed via the $(^2D_{3/2}\leftarrow{}^2P_{3/2})$ transition at 235.336 nm, the excited state by the $(^2P_{1/2}\leftarrow{}^2P_{1/2})$ transition at 235.205 nm.[21,22] Typically the dye laser was scanned over a range of ±0.003 nm around the Cl atom transition accounting for the Doppler broadening. Signals were digitized by time-to-digital converters, accumulated over 2×10^5 laser shots, and saved online by a personal computer. Details of the analyzing procedure are described elsewhere.[16]

The PSD includes a delay-line anode introduced into the spectrometer chamber right behind the double stage microchannel plates. The PSD allows one to monitor all three components of the momentum vector from the measured position of the particles on the detector and the corresponding TOF. Therefore, a full 3D velocity distribution is observed and complete information about the kinetic energy distribution and the velocity dependent β parameter can be obtained.

III. RESULTS AND DISCUSSION

Upon excitation at 235 nm the photodissociation of S_2Cl_2 may proceed via different decay channels which are well characterized by Speth *et al.*[1] As we probe Cl and Cl* photoproducts, two decay channels will be discussed in the following, i.e., reaction (1), which is called the three-body decay channel, and reaction (2), which is named radical or two-body decay channel:

$$S_2Cl_2\rightarrow S_2+2Cl, \quad \Delta H^0=(383\pm4)\ \text{kJ/mol}, \tag{1}$$

$$S_2Cl_2\rightarrow S_2Cl+Cl, \quad \Delta H^0=(214\pm10)\ \text{kJ/mol}. \tag{2}$$

The dissociation enthalpies were calculated from the standard enthalpies of formation $(\Delta_f H^0)$[23] of the molecules and radicals involved in the process and the errors were calculated according to the given errors of the individual standard enthalpies. The enthalpies were calculated for the spin–orbit ground state Cl. The ΔH^0 required for formation of one or two Cl* atoms is higher by 10.6 and 21.2 kJ/mol, respectively.

In the following, five aspects characterizing the photodissociation dynamics will be discussed: the spin–orbit branching ratio, the velocity distribution, the anisotropy parameter β, the maximal lifetimes of the excited states and the translational energy disposal E_T/E_{avl} via the different decay channels.

A. Spin–orbit branching ratio

The spin–orbit branching ratio was obtained by scanning the laser over the two resonance transitions of Cl and Cl*. The measurements were repeated at different laser light intensities. Integrating the area under the Doppler profiles results in a signal ratio S(Cl*)/S(Cl) of 0.50 ± 0.04. Taking the ratio of transition probabilities B of 1.06[22] into account we determined a Cl* yield of $\phi(\text{Cl}^*)=0.35\pm0.03$, where ϕ is defined as the ratio of the number of excited state atoms $P(\text{Cl}^*)$ to the total number of released chlorine atoms: $\phi(\text{Cl}^*)=P(\text{Cl}^*)/[P(\text{Cl})+P(\text{Cl}^*)]$. The branching ratios given by Tiemann *et al.*[24] (0.17) and Park *et al.*[8] (0.21) at 248 nm are somewhat lower, which is probably due to the different excitation wavelengths as Park *et al.*[8] concluded that the relative yield as well as the total Cl atom production of the S_2Cl_2 molecule varied with the wavelength studied.

B. Speed distribution

In Fig. 3 the speed distributions and the speed dependent anisotropy parameter β for Cl and Cl* are presented. This one-dimensional presentation is obtained via integration of the 3D data. Cl in its ground state is mainly produced at low speeds and peaks at 1200 m/s. Only a tail is observed in the high speed region above 2000 m/s. The bimodal character is more pronounced for spin excited Cl* where the two speed regions are clearly separated. Here, the bimodal character unambiguously divides the speed distribution in two parts, where Cl* is mainly released with high kinetic energy. The speed distribution of slow Cl* atoms which are a minor contribution peaks at 1500 m/s, whereas the peak for the fast atoms is at 2700 m/s. The small shoulder above 3600 m/s belongs to a small contribution of ^{37}Cl. The two speed regions correlate with the two different decay channels (1) and (2), where the energetic border between the two channels with respect to the dissociation enthalpies is at 2250 m/s. Accordingly, the fast Cl and Cl* atoms are released via the

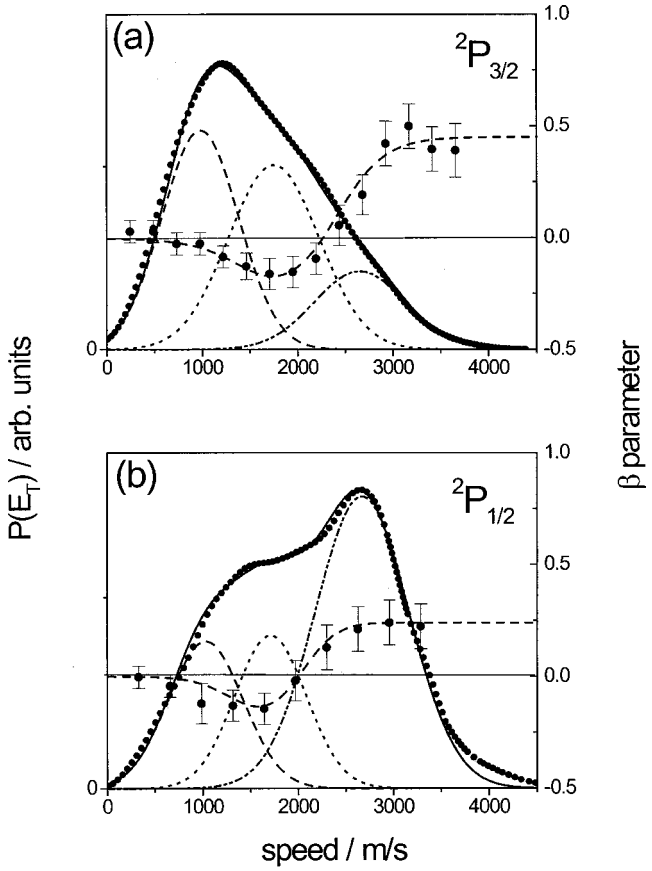

FIG. 3. Speed distribution for (a) ground state Cl($^2P_{3/2}$) and (b) excited state Cl*($^2P_{1/2}$) atoms produced in the photodissociation of S_2Cl_2 at 235 nm. The dependence of the β parameter on the Cl fragment kinetic energy (right scale) is shown by curves with error bars. In addition, the fit of the speed dependent β parameter (dashed line) for ground state Cl($^2P_{3/2}$) (a) and excited state Cl*($^2P_{1/2}$) (b) to the experimentally observed data (closed circles) on the assumption of two underlying decay mechanisms. Three Gaussians were fitted to the trimodal speed distribution. One describes the fast chlorine fragments produced in a two-body decay with a β parameter of 0.45 and 0.24 for Cl and Cl*, respectively. The other two Gaussians describe the three-body decay with a β parameter of -0.25 for the chlorine fragment released in the first step and a β parameter of zero for the slow chlorine fragment released in the second step.

radical decay channel (2) and the slow Cl and Cl* atoms are released via the three-body decay channel (1). In the case of ground state Cl the contributions of the radical and the three-body decay channel are estimated to be 17% and 83%, respectively, whereas in the case of excited state Cl* the contributions are found to be 55% and 45% for the radical and three-body decay, respectively. Detailed information of the speed distributions for Cl and Cl* is given in Table I.

C. Anisotropy parameter β and lifetimes of the excited states

The spatial fragment distribution $P(v,\theta) \propto f(v)(1+\beta(v)P_2(\cos\theta))$[25,26] is characterized by the velocity dependent anisotropy parameter $\beta(v)$ ranging from -1 (perpendicular transition) to $+2$ (parallel transition), where θ is the angle of the polarization vector of the dissociating laser with the product recoil velocity vector, and P_2 is the second Legendre polynomial: $P_2(x)=\frac{1}{2}(3x^2-1)$.

The curve shape of the speed dependent β parameter has a trimodal character for both ground and excited chlorine atoms. At low velocities (<500 m/s) the β value is close to zero, decreasing to a value of -0.15 with increasing speed up to 1750 m/s. The β value increases strongly above 2000 m/s to a value of 0.45 ± 0.12 and 0.24 ± 0.12 for Cl and Cl*, respectively. In the case of Cl* the change from -0.15 to $+0.24$ at about 2000 m/s correlates with the determined limit in the speed distribution which divides the bimodal speed distributions in two parts. Agreeing with the above-given suggestion that the bimodal character in the speed distribution reflects the different decay channels, the dependence of the β values on the speeds supports this view and gives us an insight into the dynamics of the photodissociation.

We will start our study for ground state Cl. At high velocities the Cl atoms have to be released via a two-body decay for energetic reasons where the electronic transition leads to a positive β parameter of 0.45 ± 0.12. This positive β value suggests that the initially excited state is of ^1A symmetry, because the transition dipole moment μ for the $^1A \leftarrow {}^1A$ transition is oriented parallel to the C_2 axis, which means perpendicular to the line connecting the two S atoms and bisecting the Cl–Cl angle. The geometry and the corresponding dipole moments are shown in Fig. 2. A theoretical limit of 0.48 for the β parameter for instantaneous decay is estimated from the ground state symmetry with a S–S–Cl bond angle of 45.5°. If only rotation of the parent molecules about its major principal axis is responsible for the reduction of the β parameter, the lifetime τ can be estimated based on the relationship:[27]

$$\tau = \frac{\eta}{\omega_A}, \tag{5}$$

where

$$\beta_{\text{exp}} = P_2(\eta)\beta^*, \quad \omega_A = \sqrt{\frac{kT}{I_A}}.$$

Here η is the angle between the velocity vector that would result if the molecules were not rotating and the velocity vector that actually results, ω_A is the angular rotational frequency, β_{exp} the experimentally observed anisotropy parameter, and β^* its theoretical limit. Assuming room temperature of 300 K, with $I_A \approx 7\times10^{-45}$ kg m^2 the mean rotational frequency $\omega_A \approx 8\times10^{11}$ s^{-1}, which corresponds to an upper limit of the lifetime τ of 270 fs from the experimental β_{exp} value of 0.45.

In order to extract the β parameters belonging to the speed region below 2500 m/s and therefore to the three-body decay, three Gaussians were fitted to both the Cl and Cl* speed distributions. As the β parameter is bimodal in the speed region below 2500 m/s, it is expected that the three-body decay occurs in a sequential way. Consequently one Gaussian was fitted to the high speed region (>2500 m/s), describing the two-body decay and two Gaussians were fitted to the low speed region (<2500 m/s), describing both steps of the sequential decay: (1a) $S_2Cl \rightarrow S_2C + Cl$ and (1b) $S_2Cl \rightarrow S_2 + Cl$. The Gaussian fits are also shown in Fig. 3. The contributions of the Gaussians are used to simulate the

TABLE I. Characteristic data describing the speed distribution, the β parameter of the Cl and Cl* fragments, and the kinetic energy release in the photodissociation of S_2Cl_2. The kinetic energy release is determined for the two- and three-body decay separately. The analysis consists of three Gaussians assuming a two-body decay (2BD) and a sequential three-body decay (3BD). The calculation of E_{avl} is based on an initial internal energy content of the S_2Cl_2 molecule of 8 kJ/mol at room temperature.

							Gaussian contribution	
Fragments	Type	Decay channel	E_{avl} (kJ/mol)	$\langle E_T \rangle$ (kJ/mol)	$f_r = \langle E_T \rangle / E_{avl}$	β	Center (m/s)	Full width at half maximum (m/s)
Cl	2BD	$S_2Cl_2 \rightarrow S_2Cl + Cl$	302	166±10	0.55±0.03	0.45±0.12	2650	950
	3BD	(a) $S_2Cl_2 \rightarrow S_2Cl + Cl$	136	68±10	0.50±0.03	−0.25±0.07	1750	950
		(b) $S_2Cl \rightarrow S_2 + Cl$				0±0.05	980	800
Cl*	2BD	$S_2Cl_2 \rightarrow S_2Cl + Cl$	292	169±10	0.58±0.03	0.24±0.12	2670	980
	3BD	(a) $S_2Cl_2 \rightarrow S_2Cl + Cl$	126	64±10	0.51±0.03	−0.25±0.07	1710	750
		(b) $S_2Cl \rightarrow S_2 + Cl$				0±0.05	1030	780

observed curve shape of the β dependence on the speed. Since the fit functions overlap in the medium energy range, the β parameter is accordingly reduced. The obtained simulation is shown in Fig. 3. The best values for the β parameters are 0, −0.25, and 0.45 for ground state chlorine describing slow and intermediate Cl via three-body decay and fast Cl via two-body decay, respectively. In the case of excited state Cl* the values are 0, −0.25, and 0.24, respectively. From the negative β parameter in the low speed range it can be concluded that the three-body decay proceeds via an excited state of ^1B symmetry. The value of −0.25 is in very good agreement with former translational spectroscopy measurements at 193 nm by Lee *et al.*,[12] who observed that S_2Cl_2 decays rapidly in S_2 and 2Cl with a β parameter of −0.3 on an excited ^1B state.

These observations hint at a fast dissociation, where the molecule S_2Cl_2 decays into two fragments on an excited ^1A state and mainly into three fragments on an excited ^1B state. This is supported by the overall shape of the absorption spectrum which is smooth, displaying no structure on a typical scale for vibrational spacing.[1] The continuous absorption is a good indication that direct dissociative processes take place in this region.

In the case of excited state Cl* the observed β parameter in the high speed region is 0.24±0.12. The decrease of the β parameter in comparison with the limiting value may hint at a small contribution of the excited ^1B state associated with the three-body decay releasing fast Cl* atoms. This contribution is not unlikely since a mixed excitation at 235 nm can be expected due to the location at the high-energy end of the strong absorption at 256 nm. By the reduction of the β parameter the contribution of fast Cl* being released via a ^1B state could be estimated to be ~6% of the total assuming the β value of −0.25 for Cl atoms released via the ^1B state as observed for the intermediate speed Cl and Cl* atoms. Lee *et al.*[12] also favored a mixed excitation as the reason for their observed β parameter of zero for fast S_2Cl products at 248 nm. In a former study of Lee *et al.*,[9] S_2Cl_2 was photodissociated at 308 nm and the primary dissociation process $S_2Cl_2 \rightarrow S_2Cl + Cl$ proceeds via a slightly positive β parameter of 0.4±0.2 via a ^1A state through the excitation of an ($n_{Cl} \rightarrow \sigma^*_{S\text{-}Cl}$) or ($n_S \rightarrow \sigma^*_{S\text{-}Cl}$) transition. Lee *et al.* speculated due to the existence of many nonbonding electrons in S_2Cl_2 that another repulsive ^1B state may exist. Both observations are in agreement with our present measurements. At 308 nm the Cl photoproducts were exclusively released via an excited ^1A surface yielding a positive β parameter of 0.4±0.2. The same β value is observed in the present measurement for the ground state Cl which is released solely via a ^1A state. At 248 nm Cl atoms were released via both excited states ^1A and ^1B with a positive and negative β parameter, respectively. Since Lee *et al.* measured the averaged β parameter, a value of zero was observed. The same value would be observed as an average at 235 nm, if there would not be the possibility to examine the speed dependence of the anisotropy parameter β.

In summary, the branching ratio of reactions (1) and (2) was measured to be 2.45:1.0 and 0.4:1.0 for Cl and Cl*, respectively. The simultaneous absorption into the different decay channels is illustrated in Fig. 4 in order to emphasize the competing dissociation channels at 235 nm. The three-body decay is found to be sequential as the second Cl atom is released isotropically with a β value close to zero, which means the intermediate S_2Cl^* lives long enough on a rotational time scale to lose the initial alignment of the parent S_2Cl_2 molecule and the second Cl atom is ejected without preferred spatial orientation.

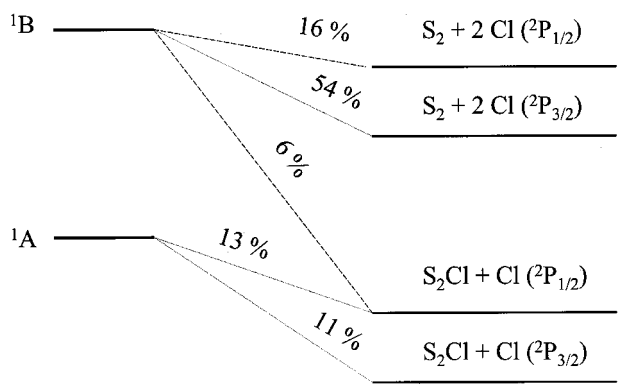

FIG. 4. Diagram illustrating the simultaneous absorption into the excited states ^1A and ^1B and the different decay channels including the spin–orbit states of Cl. The contributions refer to the total number of chlorine fragments.

IV. CONCLUSION

Using 3D imaging spectroscopy, we have measured the competing dissociation channels to release S_2Cl+Cl or S_2+2Cl in the photolysis of S_2Cl_2 at 235 nm. The main experimental findings are summarized as follows.

(1) Overall the branching ratio of reaction (2) releasing S_2Cl+Cl and reaction (1) releasing S_2+2Cl was determined to be 1.0:1.2. If the two spin–orbit states are viewed separately, the branching ratio decreases for ground state Cl to ~1.0:2.45 and increases for excited Cl* to ~1.0:0.4.

(2) The yield of Cl* in the excited spin–orbit state $^2P_{1/2}$ was found to be $\phi(\mathrm{Cl}^*)=0.35\pm0.03$.

(3) The translational energy disposal for reaction (1) was determined to be 0.53 ± 0.03 and 0.54 ± 0.03 and for reaction (2) 0.55 ± 0.03 and 0.58 ± 0.03 for Cl and Cl*, respectively.

(4) The two-body decay, releasing fast Cl (11%) and Cl* (19%), occurs mainly on a repulsive ^1A state through an electronic transition with a β parameter of 0.45 and 0.24 for Cl and Cl*, respectively. The reduced β value in the case of Cl* is probably due to mixed excitation of ^1A and ^1B, where 6% of the observed Cl* are released via the excited ^1B state.

(5) The three-body decay, releasing relatively slow Cl (54%) and Cl* (16%) atoms, occurs on a repulsive ^1B state through an electronic transition with a β parameter of -0.25 in the first step. The decay has a sequential character and the second step Cl or Cl* atoms are released isotropically ($\beta=0$).

All observations can be rationalized in terms of a simultaneous excitation on a ^1B and ^1A surface. Accordingly, the main ^1B state excitation would lead to three fragments, S_2 and two ground-state chlorine atoms. Originally from the ^1B state, nonadiabatic coupling might be responsible for a small production of excited spin–orbit Cl atoms via two- and three-body decay. The main ^1B state excitation could be accompanied by a minor excitation of a ^1A state, quickly decaying into S_2Cl+Cl, with Cl atoms generated in both spin–orbit states in almost equal amounts.

ACKNOWLEDGMENTS

The authors are grateful to Dr. R. Aures for numerous stimulating discussions. These studies were generously supported by the Fonds der Chemischen Industrie, the Alexander von Humboldt Stiftung, and the German–Israeli Foundation (GIF). Financial support by the Deutsche Forschungsgemeinschaft is gratefully acknowledged.

[1] R. S. Speth, R. Niemann, and E. Tiemann, Chem. Phys. **229**, 309 (1998).
[2] F. Feher and H. Münzer, Chem. Ber. **96**, 1131 (1963).
[3] H. P. Koch, J. Chem. Soc. **1949**, 394.
[4] B. Beagley, G. H. Eckersley, D. P. Brown, and D. Tomlinson, Trans. Faraday Soc. **65**, 2300 (1969).
[5] I. Tokue, A. Hiraya, and K. Shobatake, Chem. Phys. Lett. **153**, 346 (1988).
[6] S. A. Chasovnikov, A. I. Chichinin, and L. N. Krasnoperov, Chem. Phys. **116**, 91 (1987).
[7] E. Tiemann, H. Kanamori, and E. Hirota, J. Mol. Spectrosc. **137**, 278 (1989).
[8] J. Park, Y. Lee, and G. W. Flynn, Chem. Phys. Lett. **186**, 441 (1991).
[9] Y. R. Lee, C. L. Chiu, and S. M. Lin, Chem. Phys. Lett. **216**, 209 (1994).
[10] C. Chiu and H. Chang, Spectrochim. Acta, Part A **50**, 2239 (1993).
[11] J. Lindner, R. Niemann, and E. Tiemann, J. Mol. Spectrosc. **165**, 358 (1994).
[12] Y. R. Lee, C. L. Chiu, E. Tiemann, and S. M. Lin, J. Chem. Phys. **110**, 6812 (1999).
[13] C. Maul and K.-H. Gericke, Int. Rev. Phys. Chem. **16**, 1 (1997).
[14] J. Park, Y. Lee, J. F. Hershberger, J. M. Hossenlopp, and G. W. Flynn, J. Am. Chem. Soc. **114**, 58 (1992).
[15] A. Chichinin, T. Einfeld, C. Maul, and K.-H. Gericke, Rev. Sci. Instrum. **73**, 1856 (2002).
[16] T. Einfeld, A. Chichinin, C. Maul, and K.-H. Gericke, J. Chem. Phys. **116**, 2803 (2002).
[17] S. E. Sobottka and M. B. Williams, IEEE Trans. Nucl. Sci. **35**, 348 (1988).
[18] O. Jagutzki, V. Mergel, K. Ullmann-Pfleger, L. Spielberger, U. Meyer, R. Dörner, and H. Schmidt-Böcking, *Fast Position and Time-Resolved Read-Out of Micro-Channelplates with the Delay-Line Technique for Single Particle and Photon Detection*, edited by M. R. Descours and S. S. Shen, Imaging Spectroscopy Vol. IV (San Diego, CA, 1998), p. 322.
[19] M. Lampton, O. Siegmund, and R. Raffanti, Rev. Sci. Instrum. **58**, 2298 (1987).
[20] J. Danielak, U. Domin, R. Kepa, M. Rytel, and M. Zachwieja, J. Mol. Spectrosc. **181**, 394 (1997).
[21] S. Arepalli, N. Presser, R. Robie, and R. Gordon, Chem. Phys. Lett. **108**, 88 (1985).
[22] P. M. Regan, S. R. Langfold, D. Ascenzi, P. A. Cook, A. J. Orr-Ewing, and M. N. R. Ashfold, Phys. Chem. Chem. Phys. **1**, 3247 (1999).
[23] M. W. Chase, J. Phys. Chem. Ref. Data Monogr. **9**, I+II (1998).
[24] E. Tiemann, H. Kanamori, and E. Hirota, Annual Review, Institute for Molecular Science, Okazaki, Japan, 1988.
[25] R. N. Zare, Mol. Photochem. **4**, 1 (1972).
[26] M. Mons and I. Dimicoli, J. Chem. Phys. **90**, 4037 (1989).
[27] G. E. Busch and K. R. Wilson, J. Chem. Phys. **56**, 3638 (1972).